

Theoretical Study of Carbon Clusters in Silicon Carbide Nanowires

J. M. Morbec^{1,*} and R. H. Miwa²

¹*Instituto de Ciências Exatas, Universidade Federal de Alfenas, CEP 37130-000, Alfenas, MG, Brazil*

²*Instituto de Física, Universidade Federal de Uberlândia,
Caixa Postal 593, CEP 38400-902, Uberlândia, MG, Brazil*

(Dated: February 23, 2024)

Using first-principles methods we performed a theoretical study of carbon clusters in silicon carbide (SiC) nanowires. We examined small clusters with carbon interstitials and antisites in hydrogen-passivated SiC nanowires growth along the [100] and [111] directions. The formation energies of these clusters were calculated as a function of the carbon concentration. We verified that the energetic stability of the carbon defects in SiC nanowires depends strongly on the composition of the nanowire surface: the energetically most favorable configuration in carbon-coated [100] SiC nanowire is not expected to occur in silicon-coated [100] SiC nanowire. The binding energies of some aggregates were also obtained, and they indicate that the formation of carbon clusters in SiC nanowires is energetically favored.

PACS numbers: 71.15.Nc, 73.22.-f, 61.72.J-

I. INTRODUCTION

Silicon carbide (SiC) is a wide-band-gap semiconductor with excellent physical, electronic and mechanical properties¹ such as high thermal conductivity, high breakdown field, low density, high saturation velocity, high mechanical strength, and stability at high temperature. These exceptional features make SiC a promising candidate to replace silicon in electronic devices operating in high-power, high-frequency, and high-temperature regimes.²

In the last years, SiC nanostructures (like nanospheres,³ nanosprings,⁴ nanowires⁵ and nanotubes⁶) have been successfully synthesized, and several theoretical and experimental works^{3–11} have been performed to investigate their structural and electronic properties. The unique features of SiC combined with quantum-size effects make the SiC nanostructures interesting materials for nanotechnology applications. For instance, SiC nanowires and nanotubes have been considered as candidates for hydrogen storage nanodevices⁸ and for building blocks in molecular electronic applications.¹² In particular, silicon carbide nanowires (SiC NWs) have excellent field emission properties,¹³ high mechanical stability and high electrical conductance,⁷ and could be used as nanoscale field emitters or nanocontacts in harsh environments.

Some optical and electronic properties of semiconductors may be modified by the presence of defects. The most common defects in SiC are vacancies, interstitials, antisites and clusters. These defects are mainly formed during the growth process and ion implantation of dopants. Vacancies and interstitials of C and Si in 3C-, 4H- and 6H-SiC bulks have been thoroughly investigated in theoretical and experimental works.^{14–19} These investigations have showed that the C and Si vacancies are electron and hole traps,^{16–19} and that C and Si interstitials have higher mobility than vacancies, although the mobility of point defects in SiC is reduced as compared to

another semiconductors (like silicon).¹⁴ The high mobility of carbon interstitials favors the formation of carbon-interstitial clusters. Using *ab initio* methods, Gali et al.²⁰ systematically investigated small clusters of carbon interstitials and antisites in 3C- and 4H-SiC bulks, and verified that the formation of carbon aggregates is energetically favored.

In spite of some theoretical studies on carbon aggregates in SiC bulk,^{20–22} the investigation of carbon clusters in SiC NWs is very scarce. Motivated by the lack of studies on C aggregates in SiC NWs and by their energetically favorable formation in SiC bulk, in this work we performed an *ab initio* study of small carbon clusters in SiC NWs. We considered hydrogen-passivated SiC NWs grown along the [111] and [100] directions and examined clusters with interstitial and antisites carbon atoms. The formation energies of these clusters were determined as a function of the C concentration. We calculated the binding energies of some aggregates, and our results indicate that the formation of carbon clusters in SiC nanowires is energetically favored. Besides [111] and [100] SiC NWs, the carbon clusters were also investigated in 3C-SiC bulk, in order to compare the effect of C defects in SiC bulk and NW.

II. METHODOLOGY

In this work we present *ab initio* calculations based on density functional theory²³ (DFT) carried out by using the SIESTA code.²⁴ We used local spin-density approximation^{25–27} (LSDA) for the exchange-correlation functional and norm-conserving fully-separable pseudopotentials²⁸ to treat the electron-ion interactions. The Kohn-Sham orbitals were expanded using a linear combination of numerical pseudoatomic orbitals²⁹ and a double-zeta basis set with polarization functions³⁰ (DZP) was employed to describe the valence electrons.

The 3C-SiC bulk, and the [111] and [100] SiC NWs, were modeled within the supercell approach, with 128, 232 and 279 atoms, respectively. The SiC NWs were constructed from the 3C-SiC structure and the dangling bonds of their surfaces were saturated with hydrogen atoms. Due to the periodic boundary conditions, a vacuum region of about 10 Å was used to avoid interactions between a NW and its image. We have considered axial lengths (along the NW growth direction) of about 15.2 and 13.2 Å for the [111] and [100] SiC NWs, respectively. The geometries were optimized using the conjugated gradient scheme, within a force convergence criterion of 0.05 eV/Å. The Brillouin zone was sampled by using 2 special \mathbf{k} points for 3C-SiC bulk, and 1 special \mathbf{k} point for [100] and [111] SiC NWs. We verified the convergence of our total-energy results with respect to the number of special \mathbf{k} points using up to 9 \mathbf{k} points for 3C-SiC bulk and 4 \mathbf{k} points for [100] and [111] SiC NWs.

III. RESULTS AND DISCUSSION

We examined C clusters in 3C-SiC bulk and in hydrogen-passivated SiC NWs grown along the [111] and [100] directions.^{7,31} We considered SiC NWs with diameter of about 10 Å, constructed from the 3C-SiC structure.^{5,32} For [100] SiC NWs, two kinds of wires were studied: carbon-coated [100] SiC NW and silicon-coated [100] SiC NW, whose surfaces are, respectively, carbon and silicon terminated. Figure 1 presents the cross-section view of the structural models of carbon-coated [100] SiC NW [Fig. 1(a)], silicon-coated [100] SiC NW [Fig. 1(b)] and [111] SiC NW [Fig. 1(c)]. Note that the [111] SiC NW surface has the same number of Si and C atoms.

Eight C defects were investigated³³ in the present work (see Fig. 2): C_{Si} (carbon antisite), $C - C$ ($\langle 100 \rangle$ split of C interstitial + C site), $C - C_{Si}$ ($\langle 100 \rangle$ split of C interstitial + C antisite), $C - Si$ ($\langle 100 \rangle$ split of C interstitial + Si site), $(C - C)_i$, $2(C - C)_C$, $[(C - C)_{Si} + (C - C)_C]$, and $2(C - C)_{Si}$.

In order to examine the energetic stability of the C defects in the 3C-SiC bulk and in the [100] and [111] SiC NWs, we used the grand canonical potential at $T = 0$ K (as suggested in the Refs. 34 and 35)

$$\Omega = E_{tot} - \sum_i N_i \mu_i. \quad (1)$$

Here E_{tot} is the total energy of the considered structure, μ_i is the chemical potential of atomic specie i ($i = Si, C$ or H) and N_i is the number of atoms i in the system. In the thermodynamic equilibrium,³⁶

$$\mu_{Si} + \mu_C = \mu_{SiC}^{bulk} \quad (2)$$

and

$$\mu_{SiC}^{bulk} = \mu_{Si}^{bulk} + \mu_C^{bulk} - \Delta H(SiC), \quad (3)$$

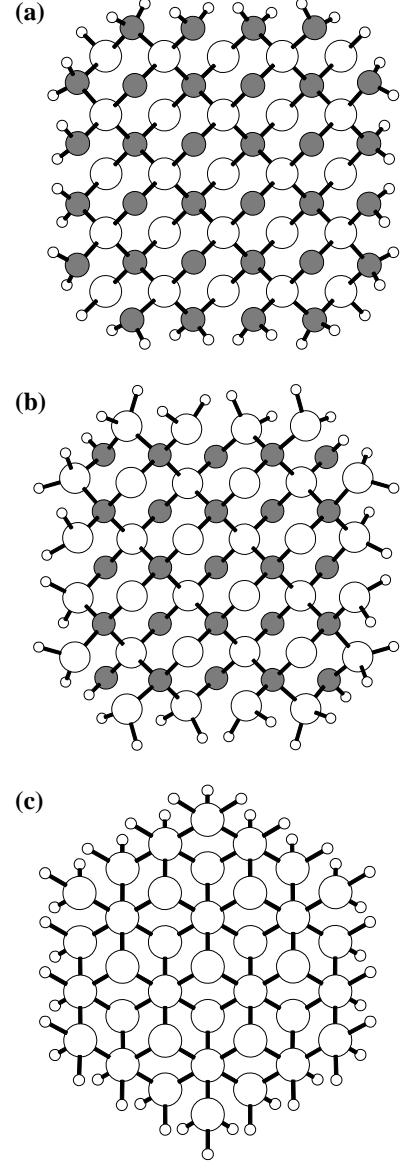


FIG. 1. Cross-section view of the structural models of (a) C-coated [100] SiC NW, (b) Si-coated [100] SiC NW and (c) [111] SiC NW. Carbon, silicon and hydrogen atoms are represented by filled, empty and small-empty circles, respectively.

where $\Delta H(SiC)$ is the formation heat of the SiC bulk. Employing diamond structure³⁷ for bulk phases of Si and C, and zincblend structure^{37,38} for SiC, we found $\Delta H(SiC) = 0.73$ eV, which is in good agreement with the experimental value $\Delta H(SiC) = 0.68$ eV.³⁹

The upper limits of μ_{Si} and μ_C are μ_{Si}^{bulk} and μ_C^{bulk} , respectively. Hence, the potential fluctuations $\Delta\mu_{Si} = \mu_{Si} - \mu_{Si}^{bulk}$ and $\Delta\mu_C = \mu_C - \mu_C^{bulk}$ are restricted to

$$- \Delta H(SiC) \leq \Delta\mu_{Si,C} \leq 0. \quad (4)$$

This range defines the C-rich (or Si-poor, where $\Delta\mu_C = 0$

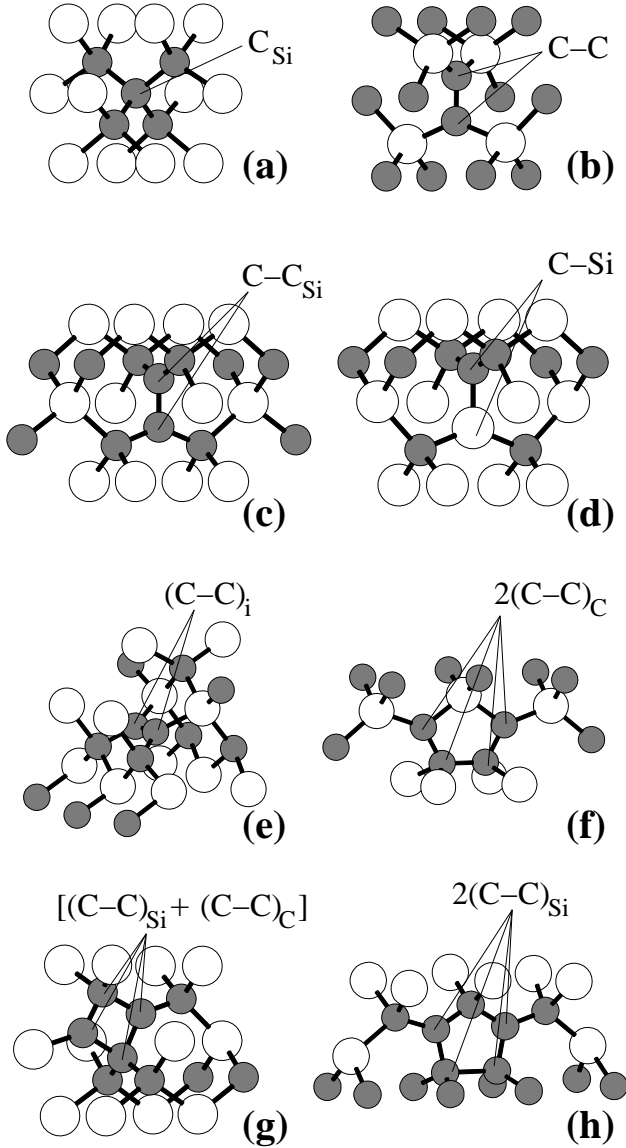


FIG. 2. Optimized geometries of the carbon defects investigated in 3C-SiC bulk and in hydrogen-passivated [100] and [111] SiC NWs. (a) C_{Si}, (b) C-C, (c) C-C_{Si}, (d) C-Si, (e) (C-C)_i, (f) 2(C-C)_C, (g) [(C-C)_{Si} + (C-C)_C], and (h) 2(C-C)_{Si}.

and $\Delta\mu_{\text{Si}} = -\Delta H(\text{SiC})$) and Si-rich (or C-poor, where $\Delta\mu_{\text{C}} = -\Delta H(\text{SiC})$ and $\Delta\mu_{\text{Si}} = 0$) limits.

In Table I we present the formation energies, relative to the pristine structures, of C defects in 3C-SiC bulk, and in hydrogen-passivated [100] and [111] SiC NWs. The two values presented in each column correspond to Si-rich (or C-poor) and C-rich limits. For 3C-SiC bulk at stoichiometric condition we found that the formation energies of C_{Si}, C-C, C-C_{Si}, (C-C)_i, 2(C-C)_{Si} and [(C-C)_{Si} + (C-C)_C] are 3.49, 7.38, 6.87, 8.79, 9.51 and 11.55 eV, respectively. These results are in good agreement with those obtained by Gali et al. in Ref. 20.

In 3C-SiC bulk, and in C-coated [100] and [111] SiC

NWs, the C_{Si} defect [Fig. 2(a)] is the energetically most favorable configuration: we find $\Delta\Omega=2.76$, 3.05, and 2.59 eV, respectively. Further formation energy comparison indicates that, upon presence of interstitial carbon atoms, C-Si [Fig. 2(d)] is energetically more stable than (C-C)_i [Fig. 2(e)], in 3C-SiC bulk, for any C concentration. We find formation energy differences ($\Delta\Omega$), between C-Si and (C-C)_i, of 1.17, 0.81 and 0.44 eV, at Si-rich, stoichiometric and C-rich conditions, respectively. That is, the formation of (C-C)_i structures is quite unlikely in 3C-SiC. Nevertheless, in both C-coated [100] and [111] SiC NWs, (C-C)_i is more favorable than C-Si at C-rich limit (by 0.21 eV in C-coated [100] SiC NW and 0.11 eV in [111] SiC NW). In this case, in contrast with the 3C SiC bulk phase, we may find C-C interstitial dimers embedded in SiC NWs [Fig. 2(e)]. However, by reducing the concentration of C atoms, we verify that C-Si becomes less stable than (C-C)_i for $\Delta\mu_{\text{C}} \geq -0.21$ and -0.11 eV, in C-coated [100] and [111] SiC NWs, respectively.

Different from C-coated [100] and [111] SiC NWs, where C_{Si} is the energetically most favorable configuration throughout the allowed range for the C chemical potential, in Si-coated [100] SiC NW the most stable defect depends on the C concentration (see Table I). At Si-rich limit C-Si is the most favorable configuration, followed by the C-C and (C-C)_i defects. However, under C-rich conditions 2(C-C)_{Si} is the most stable defect, followed by the C-C_{Si} and [(C-C)_{Si} + (C-C)_C] aggregates. Figure 3 summarizes our calculated formation energy results. The energetically most favorable defect in Si-coated [100] SiC NW is C-Si for $\Delta\mu_{\text{C}} \leq -0.43$ eV, C-C_{Si} for $-0.43 \leq \Delta\mu_{\text{C}} \leq -0.21$ eV and 2(C-C)_{Si} for $\Delta\mu_{\text{C}} \geq -0.21$ eV. At stoichiometric conditions, C-C_{Si} is the most stable configuration, followed by C-Si and (C-C)_i. We find total energy differences, under stoichiometric conditions, of 0.12 eV between C-C_{Si} and C-Si, and of 0.27 eV between C-C_{Si} and (C-C)_i.

According to Ref. 20, C-C_{Si} is energetically most favorable than C-C in 3C-SiC bulk. This result can be explained by the larger relaxation required to put two C atoms in a C site than to put two C atoms in a Si site. In the present work we observe a similar behavior [Fig. 4]: under C-rich conditions C-C_{Si} is the most stable complex with one carbon interstitial in 3C-SiC bulk and in [100] and [111] SiC NWs. However, C-C becomes energetically more stable than C-C_{Si} for low carbon concentration: $\Delta\mu_{\text{C}} \leq -0.62$ eV (in 3C-SiC bulk), -0.44 eV (in C-coated [100] SiC NW), -0.57 eV (in Si-coated SiC NW) and -0.51 eV (in [111] SiC NW). At stoichiometric conditions, C-C_{Si} is more stable than C-C by 0.52 eV (in 3C-SiC bulk), 0.16 eV (in C-coated [100] SiC NW), 0.42 eV (in Si-coated SiC NW) and 0.29 eV (in [111] SiC NW). Our result for 3C-SiC bulk is in close agreement with the result reported in Ref. 20, where C-C_{Si} is more favorable than C-C by 0.5 eV, at stoichiometric conditions.

Among the defects with two carbon interstitials, 2(C

TABLE I. Relative formation energies ($\Delta\Omega$) of carbon defects in 3C-SiC bulk, and hydrogen-passivated [100] and [111] SiC NWs. In each column the two values correspond to the Si-rich (or C-poor, where $\Delta\mu_C = -\Delta H(\text{SiC})$) and C-rich ($\Delta\mu_C = 0$) limits (Si-rich/C-rich). The energies are in eV and we used $\Delta H(\text{SiC}) = 0.73$ eV.

Defect	$\Delta\Omega$ (eV)			
	3C-SiC bulk	C-coated [100] SiC NW	Si-coated [100] SiC NW	[111] SiC NW
C_{Si}	4.22/2.76	4.51/3.05	5.26/3.80	4.05/2.59
$\text{C} - \text{C}$	7.75/7.02	6.78/6.05	4.94/4.21	7.09/6.36
$\text{C} - \text{C}_{\text{Si}}$	7.97/5.78	7.36/5.17	5.25/3.06	7.52/5.33
$\text{C} - \text{Si}$	8.35/7.62	7.53/6.80	4.64/3.91	7.45/6.72
$(\text{C} - \text{C})_{\text{i}}$	9.52/8.06	8.05/6.59	5.15/3.69	8.07/6.61
$2(\text{C} - \text{C})_{\text{C}}$	12.15/10.69	10.67/9.21	6.15/4.69	10.56/9.10
$[(\text{C} - \text{C})_{\text{Si}} + (\text{C} - \text{C})_{\text{C}}]$	10.97/8.05	9.87/6.95	6.48/3.56	9.95/7.03
$2(\text{C} - \text{C})_{\text{Si}}$	13.74/9.36	12.03/7.65	6.80/2.42	12.12/7.74

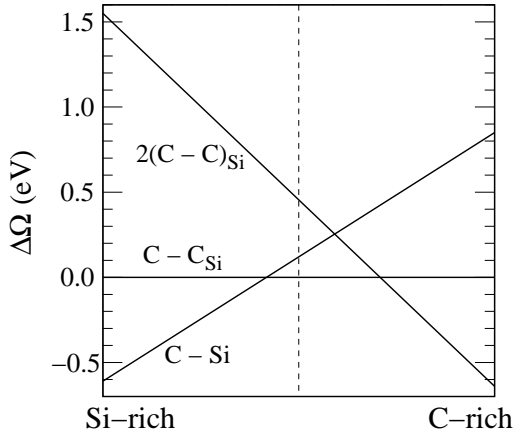


FIG. 3. Relative formation energies ($\Delta\Omega$) of the most stable C defects in Si-coated [100] SiC NW. The vertical dashed line corresponds to the stoichiometric condition.

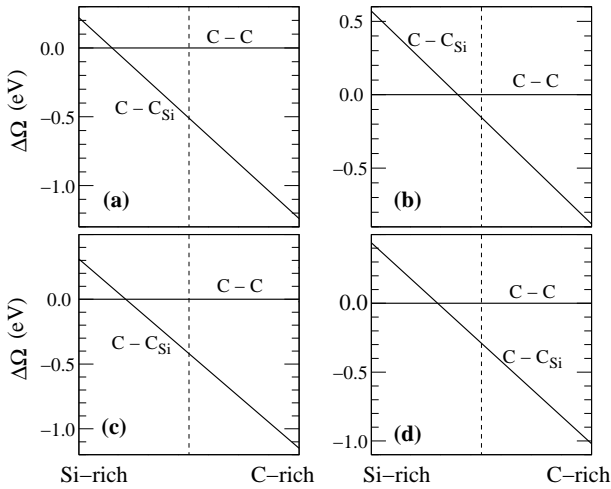


FIG. 4. Relative formation energies ($\Delta\Omega$) of $\text{C} - \text{C}$ and $\text{C} - \text{C}_{\text{Si}}$ defects in (a) 3C-SiC bulk, (b) C-coated [100] SiC NW, (c) Si-coated SiC NW and (d) [111] SiC NW. The vertical dashed lines indicate the stoichiometric condition.

$-\text{C})_{\text{Si}}$ is not expected to occur in 3C-SiC bulk, C-coated [100] SiC NW and [111] SiC NW, but is the most stable defect, at C-rich limit, in Si-coated [100] SiC NW. Besides that, at stoichiometric condition, the formation energy of $2(\text{C} - \text{C})_{\text{Si}}$ is 11.55, 9.84 and 9.93 eV in 3C-SiC bulk, C-coated [100] SiC NW and [111] SiC NW, respectively, and 4.61 eV in Si-coated [100] SiC NW. One possible reason for that is the larger relaxation of the Si-coated [100] SiC NW due to its Si-terminated surface. Hence, the $2(\text{C} - \text{C})_{\text{Si}}$ complex is created with small stress in the lattice. This surface effect is expected to disappear for larger nanowires.

We next examine the energy gain upon the formation of C clusters through the combination of interstitial C atoms. In this case, the energy gain was determined by comparing the total energies of the separated systems (E_i) and the total of a given (stoichiometrically equivalent) C cluster (E_c). We define the binding energy of the C cluster as $E^b = E_c - E_i$. Our calculated binding energies in each column correspond to the stoichiometric condition. In 3C-SiC bulk or SiC NW with a carbon antisite (C_{Si} defect), a carbon interstitial can be captured by C site, Si site or C antisite. The last process is more favorable than the first (second) one by 4.00 eV (4.60 eV) in 3C-SiC bulk, 3.93 eV (4.68 eV) in C-coated [100] SiC NW, 4.95 eV (4.65 eV) in Si-coated [100] SiC NW, and 3.62 eV (3.98 eV) in [111] SiC NW. Considering two carbon interstitials, the formation of carbon clusters is energetically favored in 3C-SiC bulk and in both [100] and [111] SiC NW. In fact, the aggregates $(\text{C} - \text{C})_{\text{i}}$ and $2(\text{C} - \text{C})_{\text{C}}$ are more stable than two isolated $\text{C} - \text{C}$ defects by 5.51 and 2.88 eV in C-coated [100] SiC NW, and by 6.11 and 3.61 eV in [111] SiC NW. Still, in Si-coated [100] SiC NW the energy gain is 13.6 eV to form $2(\text{C} - \text{C})_{\text{Si}}$ from isolated $(\text{C} - \text{C})$ and C_{Si} defects, and 3.7 eV to form $2(\text{C} - \text{C})_{\text{Si}}$ from two isolated $\text{C} - \text{C}_{\text{Si}}$. In 3C-SiC bulk these energy gains are 10.2 and 2.2 eV, respectively. Here we can infer that, in general, the formation of C clusters is quite likely in SiC NWs, in particular for thin Si-coated [100] SiC NWs. It is worth to note that, in order to get

TABLE II. Binding energies (in eV) of C defects in 3C-SiC bulk, and hydrogen-passivated [100] and [111] SiC NWs. In each column the values correspond to the stoichiometric condition.

Cluster	Binding energy (eV)			
	3C-SiC bulk	C-coated [100] SiC NW	Si-coated [100] SiC NW	[111] SiC NW
$C_{Si} + [C - C] \rightarrow [C - C_{Si}]$	-4.00	-3.93	-4.95	-3.62
$C_{Si} + [C - Si] \rightarrow [C - C_{Si}]$	-4.60	-4.68	-4.65	-3.98
$[C - C] + [C - C] \rightarrow [(C - C)_i]$	-5.98	-5.51	-4.73	-6.11
$[C - C] + [C - C] \rightarrow [2(C - C)_C]$	-3.34	-2.88	-3.72	-3.61
$[C - C_{Si}] + [C - C] \rightarrow [(C - C)_{Si} + (C - C)_C]$	-4.75	-4.27	-3.71	-4.66
$[C - C_{Si}] + [C - C_{Si}] \rightarrow [2(C - C)_{Si}]$	-2.20	-2.69	-3.70	-2.92
$2[(C - C)] + 2C_{Si} \rightarrow [2(C - C)_{Si}]$	-10.20	-10.55	-13.60	-10.16

a complete picture of the formation of C clusters, the C diffusion mechanism is an important issue, however, it is beyond the scope of the present work.

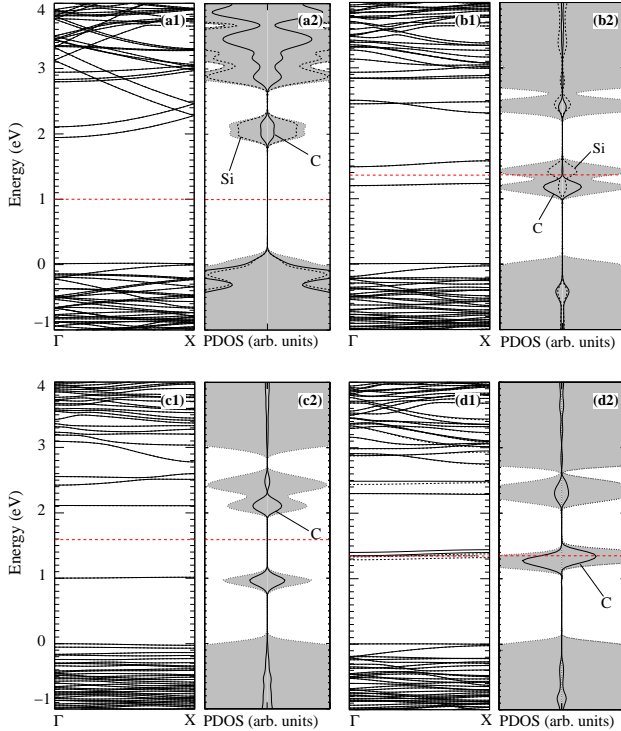


FIG. 5. (Color online) Electronic band structure and the projected density of states (PDOS) of Si-coated [100] SiC NW. (a) Pristine NW, and with the presence of defects, (b) C - Si, (c) $2(C - C)_{Si}$, and (d) $C - C_{Si}$. In the PDOS diagrams, the shaded regions correspond to the total density of states; in the electronic band structure diagrams, solid lines (dotted lines) represent the spin-up (spin-down) electronic channels. The red dashed lines correspond to the position of the Fermi level and the zero energy corresponds to the valence band maximum.

Focusing on the electronic properties, we find that similar to the 3C-SiC bulk phase,²⁰ C_{Si} is an electrically inactive defect in SiC NWs. C_{Si} does not introduce states

within the fundamental band gap. On the other hand, the formation of C clusters gives rise to electronic states lying within the energy bandgap. Figure 5(a) presents the electronic band structure and the projected density of states (PDOS) of the pristine Si-coated [100] SiC NW. The pristine system exhibits an energy bandgap (at the Γ point) of 1.98 eV, calculated within our DFT-LSDA approximation, where the highest occupied (lowest unoccupied) states are mostly composed by C 2p (Si 3p) orbitals. The formation of C clusters give rise to localized electronic states within the bandgap, as depicted in Figs. 5(b)–5(d). C - Si defect gives rise to an occupied (empty) state at 1.2 eV (1.5 eV) above the valence band maximum [Fig 5(b1)]. The dispersionless character of those states, along the ΓX direction (*i. e.* parallel to the NW growth direction), indicate that those defects states are localized around C - Si. Indeed, the PDOS diagram [Fig. 5(b2)] indicate that there is a significant contribution from the interstitial C atom to the occupied defect state, while the nearest neighbor Si atom contributes to the formation of the lowest unoccupied defect state. At the C-rich limit, the $2(C - C)_{Si}$ defect is the most favorable one. Its electronic band structure is depicted in Fig. 5(c1). We find an occupied state at 1 eV above the VBM, and three unoccupied states lying within an energy interval of 2.1 and 2.6 eV above the VBM. Those defect states are mostly localized around the interstitial C atoms [Fig. 5(c2)]. Finally, for $C - C_{Si}$ (energetically most likely at the stoichiometric condition) we find the formation of spin-unpaired states within the nearby the Fermi level, Figs. 5(d1) and 5(d2). Those defect states are localized around C interstitial atoms. In summary, different from C_{Si} defects, we verify that the formation of C clusters in Si coated [100] SiC NWs gives rise to deep states within the bandgap, which may acts as a trap to the electronic carriers.

IV. CONCLUSIONS

We performed an *ab initio* investigation of small carbon clusters in SiC bulk and NWs. We examined clusters

with carbon interstitials and antisites in 3C-SiC bulk and in hydrogen-passivated [100] and [111] SiC NWs. We observed that the composition of the SiC nanowire surface strongly influences the formation of the carbon clusters. In fact, C_{Si} is the energetically most favorable configuration in 3C-SiC bulk, and in C-coated [100] and [111] SiC NWs, but is not expected to occur in Si-coated [100] SiC NW. The energetically most stable defect in Si-coated [100] SiC NW is C – Si at Si-rich limit, C – C_{Si} at stoichiometric conditions and $2(C - C)_{Si}$ under C-rich conditions.

Comparing the total energies of the C – C and C – C_{Si} defects (in 3C-SiC bulk and in [100] and [111] SiC NWs), we find that C – C_{Si} is more stable than C – C at stoichiometric and C-rich limits. This finding is in accordance with the larger relaxation required to put two C atoms in a C site than to put two C atoms in a Si site. However,

we observed that C – C becomes energetically more stable than C – C_{Si} for low C concentration. Further total energy calculation indicate that the formation of carbon clusters in 3C-SiC bulk and in both [100] and [111] SiC NWs is energetically favored. Finally, our electronic band structure calculations indicate that (i) similar to the 3C SiC bulk phase, C_{Si} defects are electrically inactive, while (ii) in Si coated [100] NWs the C clusters gives rise to deep (localized) levels within the NW bandgap.

ACKNOWLEDGMENTS

This work received financial support from the Brazilian agencies CNPq and FAPEMIG. JMM wishes to thank I. S. Santos de Oliveira for fruitful technical discussions. All calculations were performed using the computational facilities of CENAPAD/SP.

-
- * jmmorbec@gmail.com
- ¹ W. J. Choyke, H. Matsunami, and G. Pensl (eds), *Silicon Carbide: Recent Major Advances* (Springer, Berlin, 2004).
 - ² R. Madar, *Nature* **430**, 974 (2004).
 - ³ G. Shen, D. Chen, K. Tang, Y. Qian, and S. Zhang, *Chem. Phys. Lett.* **375**, 177 (2003).
 - ⁴ D. Zhang, A. Alkhateeb, H. Han, H. Mahmood, D. N. McIlroy, and M. G. Norton, *Nano Lett.* **3**, 983 (2003).
 - ⁵ G. W. Ho, A. S. W. Wong, D. J. Kang, and M. E. Welland, *Nanotechnology* **15**, 996 (2004).
 - ⁶ X.-H. Sun, C.-P. Li, W.-K. Wong, N.-B. Wong, C.-S. Lee, S.-T. Lee, and B.-K. Teo, *J. Am. Chem. Soc.* **124**, 14464 (2002).
 - ⁷ R. Rurali, *Phys. Rev. B* **71**, 205405 (2005).
 - ⁸ P. Mélinon, B. Masenelli, F. Tournus, and A. Perez, *Nature Mater.* **6**, 479 (2007).
 - ⁹ B. Yan, G. Zhou, W. Duan, J. Wu, and B.-L. Gu, *Appl. Phys. Lett.* **89**, 023104 (2006).
 - ¹⁰ H. W. Shim, Y. Zhang, and H. Huang, *J. Appl. Phys.* **104**, 063511 (2008).
 - ¹¹ L. Sun, Y. Li, Z. Li, Q. Li, Z. Zhou, Z. Chen, J. Yang, and J. G. Hou, *J. Chem. Phys.* **129**, 174114 (2008).
 - ¹² D. Appell, *Nature* **419**, 553 (2002).
 - ¹³ Z. W. Pan, H.-L. Lai, F. C. K. Au, X. Duan, W. Zhou, W. Shi, N. Wang, C.-S. Lee, N.-B. Wong, S.-T. Lee, and S. Xie, *Adv. Mater.* **12**, 1186 (2000).
 - ¹⁴ A. Zywiec, J. Furthmüller, and F. Bechstedt, *Phys. Rev. B* **59**, 15166 (1999).
 - ¹⁵ M. Bockstedte, A. Mattausch, and O. Pankratov, *Phys. Rev. B* **69**, 235202 (2004).
 - ¹⁶ L. Torpo, R. M. Nieminen, K. E. Laasonen, and S. Pöykkö, *Appl. Phys. Lett.* **74**, 221 (1999).
 - ¹⁷ A. Gali, B. Aradi, P. Deák, W. J. Choyke, and N. T. Son, *Phys. Rev. Lett.* **84**, 4926 (2000).
 - ¹⁸ T. Umeda, J. Isoya, N. Morishita, T. Ohshima, and T. Kamiya, *Phys. Rev. B* **69**, 121201 (2004).
 - ¹⁹ G. Brauer, W. Anwand, P. G. Coleman, A. P. Knights, F. Plazaola, Y. Pacaud, W. Skorupa, J. Störmer, and P. Willutzki, *Phys. Rev. B* **54**, 3084 (1996).
 - ²⁰ A. Gali, P. Deák, P. Ordejón, N. T. Son, E. Janzén, and W. J. Choyke, *Phys. Rev. B* **68**, 125201 (2003).
 - ²¹ A. Mattausch, M. Bockstedte, and O. Pankratov, *Phys. Rev. B* **70**, 235211 (2004).
 - ²² A. Gali, N. T. Son, and E. Janzén, *Phys. Rev. B* **73**, 033204 (2006).
 - ²³ P. Hohenberg and W. Kohn, *Phys. Rev.* **136**, B864 (1964).
 - ²⁴ J. Soler, E. Artacho, J. D. Gale, A. García, J. Junquera, P. Ordejón, and D. Sánchez-Portal, *J. Phys.: Condens. Matter* **14**, 2745 (2002).
 - ²⁵ W. Kohn and L. J. Sham, *Phys. Rev.* **140**, A1133 (1965).
 - ²⁶ J. P. Perdew and A. Zunger, *Phys. Rev. B* **23**, 5048 (1981).
 - ²⁷ D. M. Ceperley and B. J. Alder, *Phys. Rev. Lett.* **45**, 566 (1980).
 - ²⁸ N. Troullier and J. L. Martins, *Phys. Rev. B* **43**, 1993 (1991).
 - ²⁹ O. F. Sankey and D. J. Niklewski, *Phys. Rev. B* **40**, 3979 (1989).
 - ³⁰ E. Artacho, D. Sánchez-Portal, P. Ordejón, A. García, and J. M. Soler, *Phys. Status Solid B* **215**, 809 (1999).
 - ³¹ R. Q. Zhang, Y. Lifshitz, D. D. D. Ma, Y. L. Zhao, Th. Frauenheim, S. T. Lee, and S. Y. Tong, *J. Chem. Phys.* **123**, 144703 (2005).
 - ³² Y. Zhang, M. N. -Gamo, C. Xiao, and T. Ando, *J. Appl. Phys.* **91**, 6066 (2002).
 - ³³ The C defects examined in this work were proposed by Gali et al. in Ref. 20.
 - ³⁴ G. X. Qian, R. M. Martin, and D. J. Chadi, *Phys. Rev. B* **38**, 7649 (1988).
 - ³⁵ J. E. Northrup and S. Froyen, *Phys. Rev. Lett.* **71**, 2276 (1993).
 - ³⁶ M. Sabisch, P. Krüger, and J. Pollmann, *Phys. Rev. B* **55**, 10561 (1997).
 - ³⁷ U. Grossner, J. Furthmüller, and F. Bechstedt, *Phys. Rev. B* **64**, 165308 (2001).
 - ³⁸ P. Käckell, B. Wensien, and F. Bechstedt, *Phys. Rev. B* **50**, 17037 (1994).
 - ³⁹ W. A. Harrison, *Electronic Structure and the Properties of Solids* (Dover, New York, 1989).